Optics and Lasers in Engineering 149 (2022) 106831

Contents lists available at ScienceDirect

Optics and Lasers in Engineering

journal homepage: www.elsevier.com/locate/optlaseng

Secondary rainbow refractometry for droplet refractive index and size measurement

Xinhao Wang, Yingchun Wu*, Qimeng Lv, Xuecheng Wu

State Key Laboratory of Clean Energy Utilization, Zhejiang University, Hangzhou 310027, China

ARTICLE INFO

Keywords:
Secondary rainbow
Refractive index
Size
Droplet measurement

ABSTRACT

Accurate measurement of droplet size, temperature and concentration in sprays is of great importance but still challenging in applications. The secondary rainbow refractometry is investigated in this work to measure refractive index and size of transparent spherical droplets, with better sensitivity than the first rainbow. Inversion algorithm of the secondary rainbow is used and validated through processing the secondary rainbow signals simulated by the Lorenz-Mie theory. The secondary rainbow refractometry is applied to measure monodispersed spherical droplets of ethanol and N-heptane with different diameters in the isothermal conditions. Measured refractive indices of both liquids are 1.3621 and 1.3950 with diameter of about 145 μm and uncertainty of size measurement is down to 1μm with RMS error of 0.3μm. Compared with results from the microscopic imaging, the maximum of deviation as well as the relative error are within several microns and 4%. This work confirms the feasibility and high accuracy of the secondary rainbow refractometry in spherical droplet size and refractive index measurement at room temperature of about $300K$.

1. Introduction

Rainbow is a kind of fascinating natural phenomena characterized by color bridge hanging in the sky, always on a sunny day after rain. Sometimes, it is possible to observe two rainbows simultaneously, and the brighter and more distinct one refers to the primary rainbow, while the other is known as the secondary rainbow. The dark region between them is the Alexander dark band. Nowadays, knowledge about rainbow technique has witnessed the development of optics, from ancient Geometric optics (GO) [1,2], Airy theory [1], Lorenz-Mie theory (LMT) [3–5], Debye theory [6,7], Nussenzveig theory to even modern quantum optics [8,9]. Theories on rainbow elucidate that the shift of angular position and the intensity distribution of rainbow signal are related to droplet refractive index (RI) and size. Rainbow refractometry for droplet diagnostics was inspired by the formation of rainbow in nature. As a typical non-intrusive optical measuring method among various optics techniques for measuring droplet size, velocity and temperature [10,11], rainbow refractometry is getting more and more attention, for its high sensitivity to the change of droplet refractive index and size, especially its applications to spray measurements.

Spray [10], a complicated phenomenon, which is of essential significance in many fields of science and engineering applications, such as spray combustion chambers, spray cooling, pharmaceutical powder and fuel injection. For example, parameter measurement of sprays can not only guide the improvement of engines [12], but also provide necessary experimental data for numerical simulation [13,14]. Liquid-gas interaction plays an important part in sprays, so in order to figure out the process of sprays and even predict the nozzle performance, droplet measuring techniques are urgent for development [15,16]. Because parameters like temperature, species can be deduced from RI, measuring refractive index and size of droplets in situ occupies an integral part of sprays investigations. There are also some appropriate models to describe the scattering pattern of non-spherical droplets, and the particle refractive index and size can be inversed in this way [17,18].

The rainbow refractometry can measure refractive index as well as size of droplets simultaneously. The angular position of rainbow signal and the light intensity distribution would alter owing to the change of droplet refractive index and size. There have hitherto been different rainbow techniques to meet great demands of various occasions comprehensively, for example, standard rainbow refractometry [19,20], global rainbow refractometry [21,22], one-dimensional rainbow refractometry [23,24] and phase rainbow refractometry [25,26]. Roth et al. [19] proposed a method to measure refractive index using the offset of the first rainbow position, to investigate liquids whose refractive index is unknown or changes due to heating and chemical processes. Van Beeck et al. [21] comprehensively introduced the concept, configuration and application of global rainbow thermometry (GRT) based on standard rainbow thermometry. Comparing experimental device and results between SRT and GRT, the pros and cons of both techniques were analyzed

* Corresponding author.
E-mail address: wuyingchun@zju.edu.cn (Y. Wu).

https://doi.org/10.1016/j.optlaseng.2021.106831
Received 21 June 2021; Received in revised form 20 August 2021; Accepted 28 September 2021
Available online 7 October 2021

[27]. Because SRT and GRT were limited to single point measurement, Wu et al. [23,24] proposed the one-dimensional rainbow thermometry (ORT) which enabled rainbow measuring technique to measure droplet refractive index and size in one dimension or a straight line. Wu et al. [25,26] took advantage of the relationship between the phase shift of high frequency ripple structure of rainbow signal and the change of particle diameter [1], and proposed phase rainbow refractometry (PRR) to measure droplet size on the micron scale and the change of droplet diameter on the nanoscale. So far, all the above rainbow refractometries have been applied in various scenarios for droplet measurements, such as measuring size, refractive index, temperature, as well as more parameters like concentration, mixing ratio, surface tension. Walker et al. [28] explained the geometric rainbow angle and angular position of the first twenty-order rainbows of water, as well as the relationship between geometric rainbow angle and refractive index. Wu et al. used global rainbow technique to study concentration and size distribution of two-component droplets [29], and investigated mixing ratio of multiple sprays using the same technique [26], with the accuracy down to 5%, in the premise of ensuring that difference of refractive index was large enough and the species of components were little. Promvongsa et al. investigated the variations of droplet diameter and composition during the evaporation of water-ethanol droplet in quiescent atmosphere using the standard rainbow refractometry [30], and applied 1D global rainbow technique to measure droplet evaporation rate and refractive index [31]. Li et al. [32] measured refractive index and size of droplets with solid inclusions through the rainbow refractometry. Lv et al. [33] applied rainbow refractometry to quantify the oscillation of droplets, and thus measured surface tension and viscosity of liquids.

Existing rainbow techniques mainly gather and inverse the first rainbow pattern, and the refracted light from first rainbow interacts with the inner surface of droplet twice. The first rainbow signal is backscattered and the intensity is high, so it is easy to collect and process signals. The difference between first and secondary rainbow is that the secondary rainbow is composed of interference with light scattering reflected on the inner surface of droplet three times. The secondary rainbow pattern of droplets with value of refractive index greater than one [34] is also backscattered and the interference from other orders rainbow is small enough to be ignored. Furthermore, in addition to high power and clear structure, the characteristic of the secondary rainbow is owning wider signal, which may mean its sensitivity is better than that of the first rainbow. So it is possible to obtain refractive index and diameter of droplets via the secondary rainbow signal. At present, the investigations concerning droplet measurement using the secondary rainbow are little. Yu et al. stimulated the optical caustics near the primary and secondary rainbow angles of oblate water droplets using a vector ray tracing model [35]. Using the generalized Lorenz-Mie theory and the Debye theory, Cao et al. [36] estimated the possibility of measuring refractive index and diameter of spherical droplets through the secondary rainbow in theory, but experimental validation was not mentioned. Nowadays, researches concerning application and inversion algorithm need further development. Actually, the secondary rainbow is undoubtedly applied to measure refractive index and particle size of spherical droplets, with some certain advantages compared with the primary rainbow refractometry, rather than limited to theoretical researches. Therefore, the secondary rainbow refractometry in this paper is used to study refractive index and size of spherical particles, in order to increase the sensitivity of rainbow technique in droplet measurement. And the size range is from tens of microns to hundreds of microns.

The optics theory and advantages of the secondary rainbow are introduced in section 2. The secondary rainbow signals of droplets with different refractive indices and diameters are simulated, and the results are derived through inversing these signals using the processing algorithm for verification in section 3, as well as the corresponding data processing algorithm. At last, the experiment setup, calibration, results and discussions of measurement are provided in section 4.1, section 4.2, section 4.3, respectively.

2. Measurement principles of secondary rainbow

Principles of the secondary rainbow are similar to that of the primary rainbow, except the interaction of the secondary rainbow between the incident light and the inner surface of droplet is three times, but for the primary rainbow it is twice. As shown in Fig. 1 (a), in which θ_{in} is the incident angle, γ is the refraction angle, θ is the scattering angle and p represents times that the incident light is refracted or reflected with the inner surface of droplets. The functional relation between θ and θ_{in}, γ, p is as follows [1,28], in which n is droplet refractive index,

$$\theta = 2\theta_{in} - 2p\gamma + (p-1)\pi. \tag{1}$$

According to the Debye decomposition, the interference light of the secondary rainbow mainly consists of four parts, as shown in Eq. 2,

$$I_{sec}^2 \approx \left|U_{\text{Debye}}^{p=0} + U_{\text{Debye}}^{p=3} + \sum_{p\neq 0,3} U_{\text{Debye}}\right|^2 = \underbrace{U_{\text{Debye}}^{p=3}\,\overline{U_{\text{Debye}}^{p=3}}_{\text{Airy}}}_{} + \underbrace{\left(U_{\text{Debye}}^{p=3}\,\overline{U_{\text{Debye}}^{p=0}} + \overline{U_{\text{Debye}}^{p=3}}\,U_{\text{Debye}}^{p=0}\right)}_{\text{ripple}}$$
$$+ \underbrace{U_{\text{Debye}}^{p=0}\,\overline{U_{\text{Debye}}^{p=0}} + U_{\text{Debye}}^{p\neq 0,3}\,\overline{U_{\text{Debye}}^{p\neq 0,3}}}_{\text{negligible}} + \underbrace{\left(U_{\text{Debye}}^{p=0} + U_{\text{Debye}}^{p=3}\right)\overline{U_{\text{Debye}}^{p\neq 0,3}} + U_{\text{Debye}}^{p\neq 0,3}\,\overline{\left(U_{\text{Debye}}^{p=0} + U_{\text{Debye}}^{p=3}\right)}}_{\text{other interference}}. \tag{2}$$

The first one is the self-interference of refracted light ($p = 3$), which is generated by two refractions and two reflections between the incident light and the inner and outer surface of droplets, and it accounts for the Airy structure and can be explained by the Airy theory. Because of its sensitivity to refractive index at angular position, the secondary rainbow is used to measure droplet refractive index. The next one is the interference between refraction and reflection, which forms the ripple structure. Moreover, the third is the reflection on the external surface of droplets in Eq. 2. Finally, the last represents the interference of light scattering orders with the main parts of the secondary rainbow ($p = 0, p = 3$), and it is usually almost invisible. But this part could lead to the superimposition of other high frequency and low amplitude ripples, and it should be carefully taken into account in case of presentence. For instance, the interference light ($p = 0, p = 4$) appears around the angle of the main peak from the secondary rainbow signal, which is essential in the inversion of diameter and refractive index, and the main influence it brings is that its light intensity is considerable compared with the other interferences. On the basis of Lorenz-Mie theory, it is uncomplicated to receive that the light intensity of interference ($p = 0, p = 4$) is about 0.05 times the maximum of the main peak, so it could be ignored.

Fig. 1 (b) displays the simulated secondary rainbow signals of a droplet with size of 100μm and RI of 1.3620 using the Airy theory, the Lorenz-Mie theory (LMT) and the Debye decomposition combining $p = 0$ and $p = 3$, and it is easily found that the main peak, supernumerary and ripple of the secondary rainbow are identical between curves of LMT and Debye from simulation results. As illustrated in Fig. 1 (a), the relation between the angular positions of the primary and secondary rainbow signals and droplet refractive index is given below,

$$\theta_{p=2} = \pi + 2\cos^{-1}\sqrt{\frac{n^2-1}{3}} - 4\sin^{-1}\sqrt{\frac{4-n^2}{3n^2}}. \tag{3}$$

$$\theta_{p=3} = 2\pi + 6\sin^{-1}\sqrt{\frac{9-n^2}{8n^2}} - 2\cos^{-1}\sqrt{\frac{n^2-1}{8}}. \tag{4}$$

When $p = 3$, the relationship between refractive index and scattering angle is shown in the Fig. 2 (a), where $1.3 \le n \le 1.45$.

In addition to the differences of signals between the secondary rainbow and the first rainbow mentioned above, the sensitivities of the first and secondary rainbow angles to refractive index can be obtained by applying a derivative to RI, as formulated in Eq. 5 and 6,

$$\text{when} p = 2, \frac{\partial\theta_{p=2}}{\partial n} = \frac{2n}{\sqrt{(4-n^2)(n^2-1)}} - \frac{16}{n\sqrt{(4n^2-4)(4-n^2)}}. \tag{5}$$

$$\text{when} p = 3, \frac{\partial\theta_{p=3}}{\partial n} = \frac{54}{n\sqrt{(9n^2-9)(9-n^2)}} - \frac{2n}{\sqrt{(9-n^2)(n^2-1)}}. \tag{6}$$

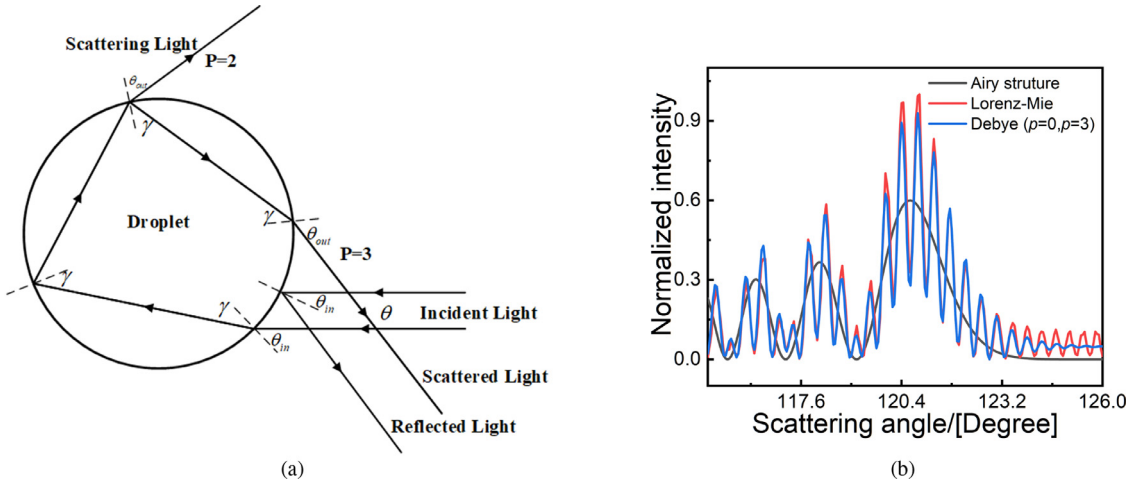

(a) (b)

Fig. 1. (a) Illusion of laser paths of the secondary rainbow. (b) a comparison of the simulated signals with the Airy theory, the Lorenz-Mie theory, the Debye theory ($p = 0, p = 3$).

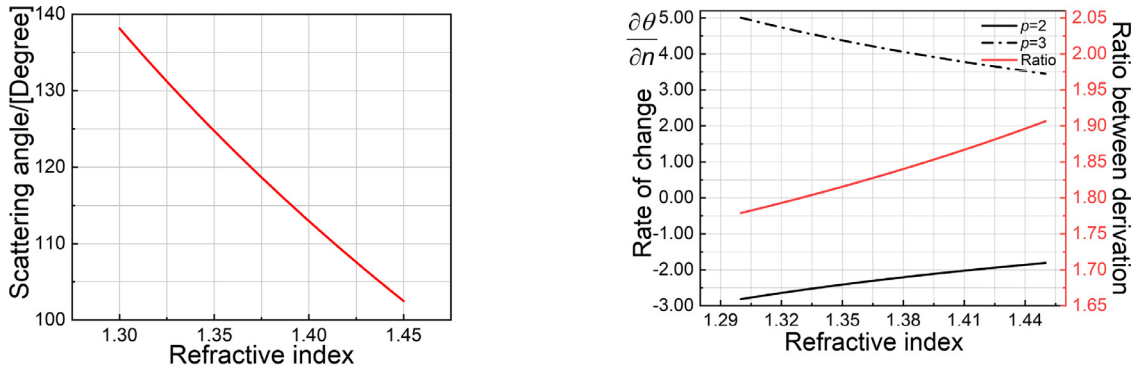

(a) (b)

Fig. 2. (a) Relationship between refractive index and scattering angle when p=3. (b) the derivation diagram of the relationship between scattering angle and refractive index when p=2 and p=3, and the ratio between values of derivation.

The range of refractive index in both formulas is limited to $1.3 \leq n \leq 1.45$, and the most common liquids would be discussed. Fig. 2 (a) depicts the curve of Eq. 4, and Fig. 2 (b) compares the curves of Eq. 5 and Eq. 6, and the ratio between values of them. As Fig. 2 (b) shows, the rate of change decreases in the curve of $p = 3$, but increases in the curve of $p = 2$ as refractive index rising. Furthermore, the gradient of the secondary rainbow signal is steeper than that of the primary rainbow signal in general, and the angle of the secondary rainbow transforms more obviously, specifically for spherical droplets. In this range of refractive index, the difference of signal gradient is large between the secondary rainbow and the primary rainbow, and then gradually decreases as the refractive index increases. For example, when $n = 1.333$, which is the RI of deionized water, absolute value of the derivative of curve from the secondary rainbow is 1.80 times that from the first rainbow, and as for ethanol, the ratio becomes 1.82. While measuring refractive index and particle size of droplets under different situations, the transform of signals can be viewed in the secondary rainbow signal more easily. Especially at the time that temperature is measured through the secondary rainbow refractometry, more subtle change would be detected and more accurate results would be given. Similarly, this feature can also be embodied in the measurement of other parameters, but this is not applicable to non-spherical droplets [37]. Therefore, an advantage of the secondary rainbow is that it has better sensitivity for the spherical droplets with regard to the changes in many parameters, like refractive index and temperature.

In order to furtherly certificate the statement that the secondary rainbow owns better sensitivity, the secondary rainbow signals are simulated under the framework of the Lorenz-Mie scattering theory. The simulated secondary rainbow signals are obtained by calculating the light scattering of a single droplet near the secondary rainbow angle and ignoring the interference caused by light scattering of different droplets. Fig. 3 (a) simulates the primary rainbow signal and the secondary rainbow signal of ethanol droplets with different diameters, where the main peak and supernumerary can be observed. As the diameter of droplet increases, the width of the main peak becomes smaller with light intensity of the secondary rainbow signal larger. Combining analog signals of the primary rainbow and the secondary rainbow in Fig. 3 (a), the angle range of the main peak from the secondary rainbow is about 4.6 degrees, and for the primary rainbow is about 2.5 degrees at the same conditions. Fig. 3 (b) shows the simulated signals of ethanol and water droplets with the same particle size, which reflects the change of scattering angle is obvious. In the secondary rainbow signal, the angle between the maximum value of peaks is 7.3 degrees, however, it is 4.0 degrees for the primary rainbow. With the same preset conditions, the simulated signal of the secondary rainbow performs better than that of the primary rainbow in the aspect of sensitivity. In conclusion, the secondary rainbow is more sensitive to the change of refractive index, particle size and other parameters of droplets than the primary rainbow.

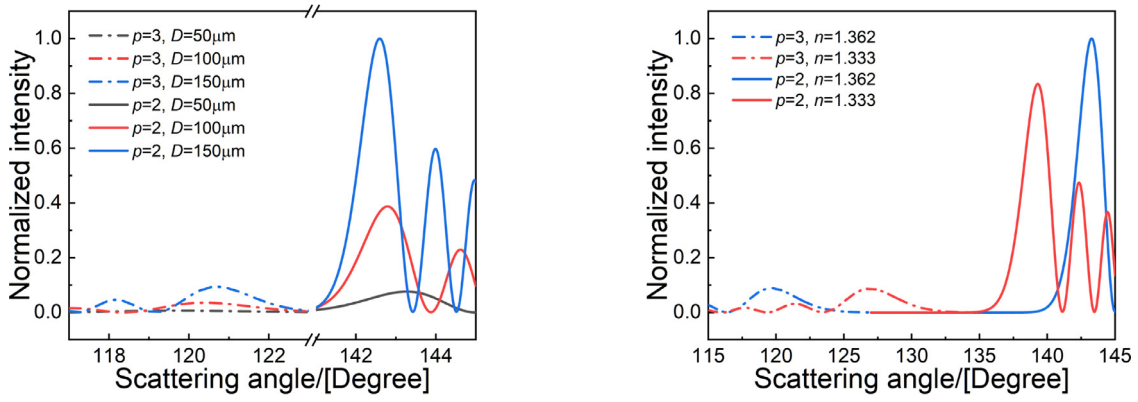

Fig. 3. (a) The primary rainbow signal and the secondary rainbow signal of ethanol droplets with different diameters (size is 50m, 100m, 150m, respectively). (b) the primary rainbow signal and the secondary rainbow signal of different droplets with the same diameter (size is 100m, RI is 1.362 and size is 100m, RI is 1.333).

3. Simulation validation

To inverse refractive index and diameter, an optimal fitting is performed between the sampled secondary rainbow signal and the theoretical one. After obtaining the secondary rainbow signal, the light intensity distribution can be transformed, recorded as the column vector E_{rb} shown as follow

$$E_{rb} = \begin{bmatrix} e_1 & e_2 & e_3 & \cdots & e_m \end{bmatrix}^T. \tag{7}$$

Assuming the composition, concentration, refractive index and other parameters of droplets are identical, and the distribution of size is non-constraint, the droplets are represented by D_{rb}. While calculating the coefficient vector T_{rb} of the secondary rainbow using Debye theory containing $p = 0$ and $p = 3$, the column vector $I_{rb}(n, \theta, d)$ represents the theoretical signal strength of the secondary rainbow,

$$I_{rb}(n,\theta,d) \cong T_{rb} \cdot D_{rb} = \begin{bmatrix} t(n,\theta_1,d) & t(n,\theta_2,d) & t(n,\theta_3,d) & \cdots & t(n,\theta_m,d) \end{bmatrix}^T \cdot D_{rb}, \tag{8}$$

where d is the size of droplet.

The interference between rainbow signals from multiple droplets is smoothly filtered out, and then ignored in the measurement area. Adopting the Non-Negative Least Squares (NNLS) method, and iteratively searching the refractive index and the size distribution, the value of $I_{rb}(n, \theta, d)$ is made closest to E_{rb},

$$\arg\min_{n,d} \left| E_{rb} - I_{rb}(n,\theta,d) \right|, \text{ s.t. } n \in \left[n_{\min}, n_{\max} \right], d \in \left[d_{\min}, d_{\max} \right]. \tag{9}$$

Brent's method [38] is applied in the process of searching optimization, and the optimized parameters can be got when difference is less than the present threshold. And this method can converge and solve more accurately and quickly, given the range of value that contains only one roots. When the absolute error between two vectors becomes minimum, the optical solution is obtained, and at this time refractive index and particle size are outputted. The Debye theory can be replaced with the Airy and Lorenz-Mie theory, and despite above three methods have differences, there is almost no effect on the measuring results.

The secondary rainbow signal is simulated with definite refractive index and size, so as to verify accuracy of the inversion algorithm, in other ways, to ensure the feasibility of the secondary rainbow refractometry. The secondary rainbow simulated signal is obtained by calculating the light scattering of a single droplet near the secondary rainbow angle and ignoring the interference caused by light scattering of different droplets. The research object of this paper is the light scattering of spherical and uniform droplets, so the Lorenz-Mie theory is used to simulate the light scattering of droplets illuminated by a laser, in order to simulate the Gaussian beam in the experiment. The influence of simulated signals is negligible, caused by other orders of rainbow on simulation, because the light intensity of other orders is ignorable compared with the secondary rainbow signal.

Fig. 4 (a) is a typical fitting between simulated signal and theoretical signal of the secondary rainbow during inversion, with inversed diameter of 60 μm and refractive index of 1.380. Both curves of signals fit well in overall, and the positions of peaks are similar. Fig. 4 (b) indicates inversed values and preset values, and only two sets of comparison values have a certain difference. The most deviation is 0.5 μm for size and 2×10^{-3} for refractive index, and the relative errors are all within 0.4%, 0.1% for diameter and RI respectively while measuring droplets with different diameters, illustrating the inversed values is extremely close to the preset values. However, it is obvious that there are some fluctuations in the diagram. The reason may be that the light scattering process is too complicated to be fully expressed through theory in actuality. As the previous researches revealed, only the beam waist was much larger than droplet size, could scattering angle be regarded as being illuminated by plane wave irradiation. In conclusion, the inversion algorithm mentioned can ensure the accuracy of the secondary rainbow refractometry. While taking the average value of the upper and lower fifty rows of pixels as the secondary rainbow signal for inversion, the average time is about a minute.

4. Experiments and results

4.1. Experimental setup

The experimental setup involved a secondary rainbow refractometry and a system of droplet generation. Uniform stable droplets were produced by a self-developed droplet generator, and diameter of droplets can be controlled. A laser beam illuminated the droplets stream, with a wavelength of 532 nm and polarization perpendicular to the observation plane, and the droplet diameter range was 120–150 μm. The backscattered light was gathered by a plane-convex lens, namely collecting lens, with focal length of 75.0 mm and diameter of 50.8 mm. An aperture, located at the imaging surface of the collecting lens, formed the spatial filter with correcting lens, so as to intercept the interference light. The second lens, imaging lens, with its imaging surface coincided with the focal plane of collecting lens, made up a Fourier imaging system with collecting lens, as shown in Fig. 5.

After the imaging lens, the light scattering was projected and recorded on the industrial camera. After calculating and adjusting in the experiment, the distance between the collecting lens, aperture, imaging lens and camera was determined to be 160 mm, 70 mm, 80 mm respectively, in the premise that measuring distance was 150 mm. The pixels of the camera were 1920×1200, and exposure time was 800 ms.

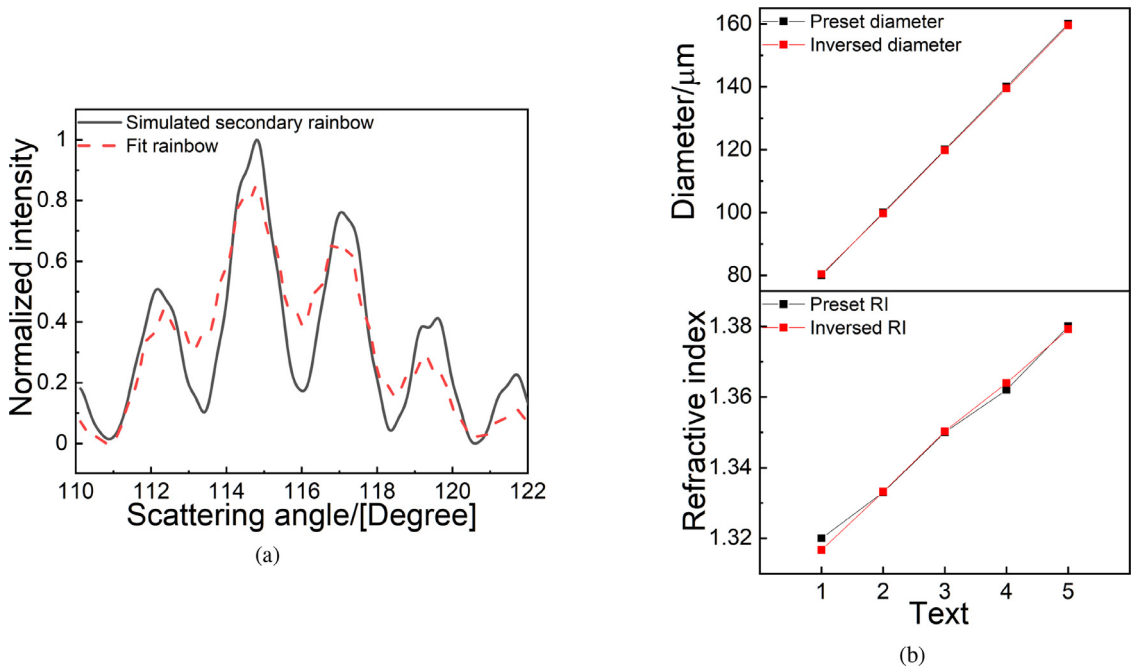

Fig. 4. (a) The fitting of simulated signal and theoretical signal of the secondary rainbow. (b) inversed values and preset values of diameters and refractive index.

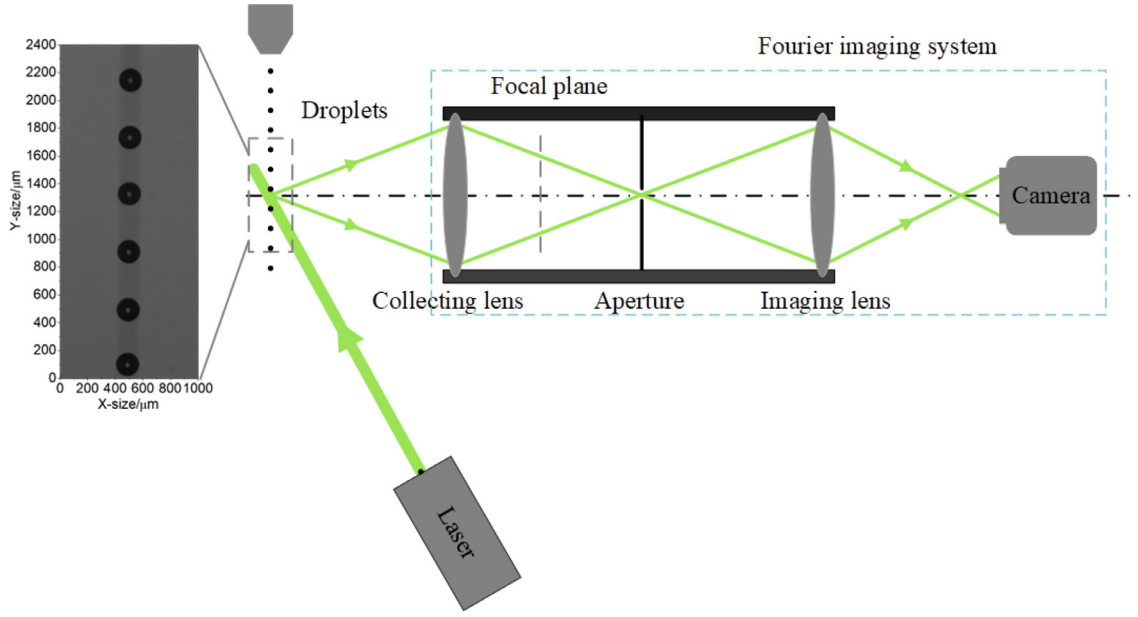

Fig. 5. Schematic diagram of secondary rainbow refractometry and droplets generation with the image from the microscopic imaging.

Since the composition of droplets was absolute ethanol, the angle between incident direction of the laser and the collection system was 141°, in which way the secondary rainbow could be imaged in the middle of industrial camera. While the secondary rainbow refractometry was working, a light source and a high-speed camera laid on both sides of droplets on an axis, and droplets images were reported by the camera directly. The position of high-speed camera and the magnification of lens were adjusted until clear droplets could be observed on the high-speed camera, as a comparative experiment of the secondary rainbow refractometry. During the experiment, the secondary rainbow signals and the droplets images were recorded under different working conditions, with droplet size varying. Fig. 5 consists of a microscopic image of signal ethanol droplet, and size can be calculated according to the numbers of pixels occupied by a droplet in the image after calibration. After measuring droplets of different situations with two techniques, measurement results between the secondary rainbow refractometry and the microscopic imaging technique are compared, in order to verify the accuracy of size measurement of the secondary rainbow refractometry. And the apparatus introduced above can also be employed to measure sprays, because the light scattering intensity is only related to the dispersion angle. When measured droplets are polydisperse, the inversion algorithm should be adjusted accordingly.

4.2. *Scattering angle-pixel calibration*

Because the relationship between scattering angle and pixel position is necessary to data inversion, it is important to obtain the scattering angle of laser corresponding to the different positions on the camera

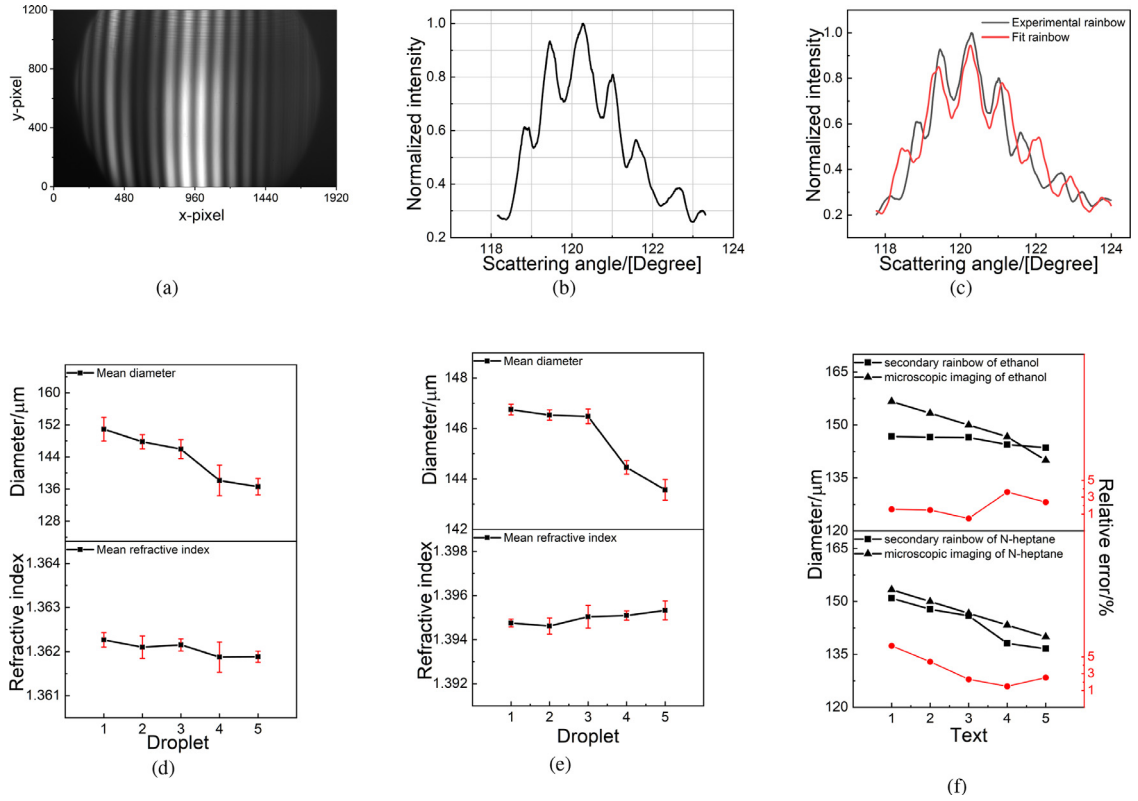

Fig. 6. (a) a secondary rainbow picture from the secondary rainbow refractometry. (b) a graph of the secondary rainbow signal after normalization. (c) the fitting of inverted signal and theoretical signal of the secondary rainbow. (d) and (e) are the diagrams of diameter and refractive index values obtained through measuring ethanol and N-heptane droplets with the secondary rainbow refractometry. (f) a comparison diagram about diameters of ethanol and N-heptane droplets using the secondary rainbow refractometry and the microscopic imaging technique.

sensor. This work adopted calibration method using mirror [29], the key point of which was that mirror was placed at the measuring point with high-precision rotating platform. Toward accurately finding the position of measuring point, two lasers were used and the measuring point was registered by the intersection point of two beams. Before calibration, turning off a laser and adding an attenuator between laser and camera were important to decrease laser intensity, in order to protect camera from damage. Mirror was being rotated from where reflector was perpendicular to the incident light until the reflected light coincided with the optical axis of the secondary rainbow signal collection system. The rotation angle and the position of reflected light on the camera were recorded respectively. Finally, combining the angle between the direction of laser emission and the optical axis of the secondary rainbow signal acquisition system, the scattering angle at the measurement point could be captured, and then the relationship between the light scattering angle and the pixels on the camera would be obtained.

4.3. Results and discussion

Fig. 6 (a) displays a secondary rainbow picture of a single ethanol droplet, where the main peak of Airy rainbow, supernumerary and ripple structure superimposed on that can be observed clearly. Fig. 6 (b) demonstrates a graph of the secondary rainbow normalized signal from the experiment. A complete secondary rainbow signal curve is obtained through taking the average value of the upper and lower twenty rows of pixels, whose center is selected as the position of laser shown on the camera during calibration. Fig. 6 (c) shows the fitting of inverted signal and theoretical signal of the secondary rainbow. The overall trends of both curves are consistent and the peaks fit well. The main discrepancy embodies in the intensity of secondary rainbow signals, which nearly makes no difference to inversing refractive index and diameter. Such fitting of two rainbow signals ensures the accuracy of the secondary rainbow refractometry.

While processing data of each condition, thirty samples selected from images of the secondary rainbow were inversed and then averaged to gain the last results. Fig. 6 (d) and (e) are diagrams of diameter and refractive index values obtained through measuring ethanol and N-heptane spherical droplets with the secondary rainbow refractometry at ambient temperature, respectively, with the root mean square (RMS) error of each parameter. When the diameter of dropets is about 145 μm, it is obvious that refractive index of ethanol droplets is 1.3621, with small fluctuation, and refractive index of N-heptane is 1.3950. All of these are identical to the known refractive index values of ethanol and N-heptane in similar conditions, because according to papers, the values are 1.3630 for ethanol at 293K [39] and 1.3911 for N-heptane at room temperature [40]. In the experiment, the average values of RMS error are 2.1×10^{-4} and 3.4×10^{-4} for ethanol and N-heptane respectively, indicating that measurement of refractive index is not influenced by the change of particle size. And the uncertainty on the refractive index is in the fourth digit for both two liquids, proving the feasibility to measure refractive index using the secondary rainbow refractometry. As for diameter measurement, the particle size values have a large difference in measuring droplets with unequal diameters for ethanol and N-heptane. The average RMS error of the N-heptane particle size measurement with five different sizes is 0.3 μm, and the uncertainty is 0.8 μm, for ethanol droplets, the RMS error is 2.6 μm, and the uncertainty is 7.2 μm. Although the measuring deviation of ethanol droplets is larger than that of N-heptane droplets, both derivations can satisfy the engineering applications. Therefore, it is verified that the accuracy and stability of the secondary rainbow refractometry to measure diameter with small deviations.

Fig. 6 (f) is a comparison diagram about diameters of ethanol and N-heptane spherical droplets at constant temperature using the secondary rainbow refractometry and the microscopic imaging technique. The values of ethanol droplet size are similar from the two techniques, and derivation is within 5μm with average relative error of 2.3%. The difference of N-heptane particle size is bigger between two methods, and the change of measurement results is smaller with the diameter varying. The maximum derivation between two methods is 10 μm, and the average relative error is 3.6%. For instance, when the result of measuring droplet size was 150.0 μm through the microscopic imaging, the sizes were 148.2 μm and 146.4 μm for ethanol and N-heptane droplets respectively through the secondary rainbow refractometry. When the value of microscopic imaging becomes 143.3 μm, the diameters are 138.1 μm and 143.6 μm for both droplets. Although the results of two techniques have a small derivation, the reliability and accuracy of the secondary rainbow refractometry to measure droplet size is considerable, taking into account measurement errors of the microscopic imaging method.

5. Conclusion

In this work, the secondary rainbow refractometry is proposed and descripted in detail from measurement principle, numerical simulation, inversion algorithm to experimental measurement. The secondary rainbow refractometry is successfully applied to measure refractive index and size of droplets, with both feasibility and accuracy verified.

- It is found that the secondary rainbow is sensitive to the change of parameters such as diameter and refractive index. Therefore, it is verified that the level of sensitivity to measure parameters of spherical droplets is higher with the secondary rainbow refractometry through simulating several droplets, and the inversion algorithm is proposed corresponding to the secondary rainbow. While processing simulated signals, the relative errors are all within 0.4%, 0.1% for diameter and RI respectively, illustrating reliability and accuracy of the inversion algorithm.
- The secondary rainbow refractometry is utilized to measure spherical droplets at room temperature with different diameters and types. The refractive indices values are 1.3621 and 1.3950 while measuring ethanol and N-heptane droplets with diameter of about 145 μm, and the RMS errors are 2.1×10^{-4} and 3.4×10^{-4}, respectively. And for diameters measurement, the average RMS error of ethanol and N-heptane particle are 0.3 μm and 2.6 μm. It is confirmed that measurement of refractive index is not influenced by the change of particle size, and it will be used to measure temperature, composition and other parameters with better sensitivity.
- The diameters measured by the secondary rainbow refractometry are compared with those obtained from the microscopic imaging method, and the relative errors of both ways are little, which are 2.3% and 3.6%. It is proved that the secondary rainbow refractometry can be applied to obtain size of droplets with high accuracy.

The secondary rainbow refractometry owns higher sensitivity while measuring refractive index and size of spherical droplets at ambient temperature. In the case of parameters with a slight change, the secondary rainbow is likely to capture and record this information. However, there is still a lack of the secondary rainbow theory that ensures accuracy and reduces time-consuming. In this paper, only one case is proved that the secondary rainbow refractometry is applied to measure a single droplet, and it is firmly believed that the secondary rainbow refractometry can be extended to be combined with the global rainbow refractometry, the one-dimension rainbow refractometry and the phase rainbow refractometry. With comprehensive and in-depth development, the secondary rainbow refractometry will be used in the measurement of refractive index and size of spherical droplets more extensively.

Declaration of Competing Interest

The authors declare that they have no known competing financial interests or personal relationships that could have appeared to influence the work reported in this paper.

CRediT authorship contribution statement

Xinhao Wang: Resources, Data curation, Writing – review & editing. **Yingchun Wu:** Methodology, Writing – original draft. **Qimeng Lv:** Data curation. **Xuecheng Wu:** Conceptualization.

Acknowlgedgments

The authors gratefully acknowledge the support from project supported by National Natural Science Foundation of China (52006193), Zhejiang Provincial Natural Science Foundation of China under Grant No. LQ19E060010, National Science and Technology Major Project (2017-V-0016-0069).

Supplementary material

Supplementary material associated with this article can be found, in the online version, at doi:10.1016/j.optlaseng.2021.106831.

References

[1] Van Beeck JPAJ, Riethmuller ML. Rainbow phenomena applied to the measurement of droplet size and velocity and to the detection of nonsphericity. Appl Opt 1996;35(13):2259–66.
[2] Bohren CF, Huffman DR. Absorption and scattering of light by small particles. John Wiley & Sons; 2008. ISBN 3527618163
[3] Adam JA. The mathematical physics of rainbows and glories. Phys Rep 2002;356(4–5):229–365.
[4] Nussenzveig HM. Diffraction effects in semiclassical scattering. Cambridge University Press; 2006.
[5] Gouesbet G, Gréhan G. Generalized lorenz-mie theories, 31. Springer; 2011.
[6] Li R, Han X, Jiang H, Ren KF. Debye series for light scattering by a multilayered sphere. Appl Opt 2006;45(6):1260–70. doi:10.1364/ao.45.001260. https://www.ncbi.nlm.nih.gov/pubmed/16523791
[7] Xu F, Lock JA, Tropea C. Debye series for light scattering by a spheroid. JOSA A 2010;27(4):671–86.
[8] Nussenzveig HM. High frequency scattering by a transparent sphere. i. direct reflection and transmission. J Math Phys 1969;10(1):82–124. doi:10.1063/1.1664764.
[9] Nussenzveig HM. High frequency scattering by a transparent sphere. ii. theory of the rainbow and the glory. J Math Phys 1969;10(1):125–76. doi:10.1063/1.1664747.
[10] Fansler TD, Parrish SE. Spray measurement technology: a review. Meas Sci Technol 2015;26(1). doi:10.1088/0957-0233/26/1/012002.
[11] Gouesbet G, Gréhan G. Laser-based optical measurement techniques of discrete particles: a review [invited keynote]. Int J Multiphase Flow 2015;72:288–97. doi:10.1016/j.ijmultiphaseflow.2014.07.001.
[12] Sick V. High speed imaging in fundamental and applied combustion research. Proc Combust Inst 2013;34(2):3509–30. doi:10.1016/j.proci.2012.08.012.
[13] Shinjo J, Umemura A. Simulation of liquid jet primary breakup: dynamics of ligament and droplet formation. Int J Multiphase Flow 2010;36(7):513–32. doi:10.1016/j.ijmultiphaseflow.2010.03.008.
[14] Rutland CJ. Large-eddy simulations for internal combustion engines a review. Int J Engine Res 2011;12(5):421–51. doi:10.1177/1468087411407248.
[15] Coghe A, Cossali GE. Quantitative optical techniques for dense sprays investigation: a survey. Opt Lasers Eng 2012;50(1):46–56. doi:10.1016/j.optlaseng.2011.07.017.
[16] Linne M. Imaging in the optically dense regions of a spray: areview of developing techniques. Prog Energy Combust Sci 2013;39(5):403–40. doi:10.1016/j.pecs.2013.06.001.
[17] Onofri FR, Ren KF, Sentis M, Gaubert Q, Pelcé C. Experimental validation of the vectorial complex ray model on the inter-caustics scattering of oblate droplets. Opt Express 2015;23(12):15768–73.
[18] Ren KF, Onofri F, Rozé C, Girasole T. Vectorial complex ray model and application to two-dimensional scattering of plane wave by a spheroidal particle. Opt Lett 2011;36(3):370–2.
[19] Roth N, Anders K, Frohn A. Simultaneous measurement of temperature and size of droplets in the micrometer range. J Laser Appl 1990;2(1):37–42.
[20] Van Beeck JPAJ, Riethmuller ML. Nonintrusive measurements of temperature and size of single falling raindrops. Appl Opt 1995;34(10):1633–40.
[21] Beeck JPAJV, Giannoulis D, Zimmer L, Riethmuller ML. Global rainbow thermometry for droplet-temperature measurement. Opt Lett 1999;24(23):1696–8.
[22] van Beeck JP, Zimmer L, Riethmuller ML. Global rainbow thermometry for mean temperature and size measurement of spray droplets. Particle & Particle Systems Characterization: Measurement and Description of Particle Properties and Behavior in Powders and Other Disperse Systems 2001;18(4):196–204.

[23] Wu X, Jiang H, Wu Y, Song J, Grehan G, Saengkaew S, et al. One-dimensional rainbow thermometry system by using slit apertures. Opt Lett 2014;39(3):638–41. doi:10.1364/OL.39.000638. https://www.ncbi.nlm.nih.gov/pubmed/24487885
[24] Wu Y, Promvongsa J, Wu X, Cen K, Grehan G, Saengkaew S. One-dimensional rainbow technique using fourier domain filtering. Opt Express 2015;23(23):30545–56. doi:10.1364/OE.23.030545. https://www.ncbi.nlm.nih.gov/pubmed/26698532
[25] Wu Y, Promvongsa J, Saengkaew S, Wu X, Chen J, Grehan G. Phase rainbow refractometry for accurate droplet variation characterization. Opt Lett 2016;41(20):4672–5. doi:10.1364/OL.41.004672. https://www.ncbi.nlm.nih.gov/pubmed/28005864
[26] Wu Y, Crua C, Li H, Saengkaew S, Mädler L, Wu X, et al. Simultaneous measurement of monocomponent droplet temperature/refractive index, size and evaporation rate with phase rainbow refractometry. J Quant Spectrosc Radiat Transfer 2018;214:146–57. doi:10.1016/j.jqsrt.2018.04.034.
[27] Beeck JPV, Riethmuller ML, Lavergne G, Biscos Y, Atthasit A. Processing droplet temperature measurement data obtained with rainbow thermometry. Proc SPIE Int Soc Opt Eng 2001;4448.
[28] Walker JD. Multiple rainbows from single drops of water and other liquids. Am J Phys 1976;44(5):421–33. doi:10.1119/1.10172.
[29] Wu X, Wu Y, Saengkaew S, Meunier-Guttin-Cluzel S, Gréhan G, Chen L, et al. Concentration and composition measurement of sprays with a global rainbow technique. Meas Sci Technol 2012;23(12). doi:10.1088/0957-0233/23/12/125302.
[30] Promvongsa J, Fungtammasan B, Gerard G, Saengkaew S, Vallikul P. A study on the evaporation of water ethanol mixture using rainbow refractometry. J Energy Resour Technol 2017;139(6). doi:10.1115/1.4037157.
[31] Promvongsa J, Vallikul P, Fungtammasan B, Garo A, Grehan G, Saengkaew S. Multicomponent fuel droplet evaporation using 1d global rainbow technique. Proc Combust Inst 2017;36(2):2401–8. doi:10.1016/j.proci.2016.08.010.
[32] Li C, Wu X-c, Cao J-z, Chen L-h, Gréhan G, Cen K-f. Application of rainbow refractometry for measurement of droplets with solid inclusions. Optics & Laser Technology 2018;98:354–62. doi:10.1016/j.optlastec.2017.07.026.
[33] Lv Q, Wu Y, Li C, Wu X, Chen L, Cen K. Surface tension and viscosity measurement of oscillating droplet using rainbow refractometry. Opt Lett 2020;45(24):6687–90. doi:10.1364/OL.412498. https://www.ncbi.nlm.nih.gov/pubmed/33325871
[34] Ouattara M, Lamadie F, Sentis MP, Onofri FR. Droplet sizing and mixture fraction measurement in liquid–liquid flows with rainbow-angle diffractometry. Appl Opt 2017;56(29):8109–20.
[35] Yu H, Shen J, Tropea C. Optical caustics associated with the primary and the secondary rainbows of oblate droplets. In: International Conference on Optical Particle Characterization (OPC 2014), 9232. International Society for Optics and Photonics; 2014. p. 923207.
[36] Cao Y, Wang W, Yu H, Shen J, Tropea C. Characterization of refractive index and size of a spherical drop by using gaussian beam scattering in the secondary rainbow region. J Quant Spectrosc Radiat Transfer 2020;242. doi:10.1016/j.jqsrt.2019.106785.
[37] Onofri F, Bergounoux L, Firpo J, Mesguish-Ripault J. Velocity, size and concentration measurements of optically inhomogeneous cylindrical and spherical particles. Appl Opt 1999;38(21):4681–90.
[38] Press WH, Vetterling WT, Teukolsky SA, Flannery BP. Numerical recipes, 818. Cambridge university press Cambridge; 1986.
[39] Sani E, DellOro A. Corrigendum to “optical constants of ethylene glycol over an extremely wide spectral range” [opt. mater. 37 (2014) 36–41]. Opt Mater (Amst) 2015;48. doi:10.1016/j.optmat.2015.06.039.
[40] Kerl K, Varchmin H. Refractive index dispersion (rid) of some liquids in the uv/vis between 20°C and 60°C. J Mol Struct 1995;349:257–60.